Demonstration of a High-Capacity Cryocooler for Zero Boil-Off Cryogen Storage in Space

M. Zagarola, J. Breedlove, K. Cragin

Creare Incorporated
Hanover, NH 03755

ABSTRACT

NASA is planning a ground demonstration of the thermal control system for zero boil-off liquid oxygen storage. The purpose of this demonstration is to advance the technology readiness level of the overall system to 5/6. A key sub-system is the cryogenic refrigerator that intercepts parasitics and provides pressure control for the cryogen. Turbo-Brayton cryocoolers are ideal for these systems because they scale well to the high capacities associated with cryogen storage and they can interface directly with a distributed cooling network located on a cryogen tank, obviating the need for a separate circulator. In support of NASA's program, Creare developed and demonstrated a single-stage cryocooler that provides up to 20 W of refrigeration at 90 K. The cryocooler comprises components built for a prior flight demonstration program that were configured to meet the specific requirements of a cryogen storage system. The subjects of this paper are the cryocooler design, the interfaces with the cryogen storage tank, results from the cryocooler performance test conducted at Creare prior to delivery of the cryocooler, and scaling of the technology to higher cooling capacities to support future missions.

INTRODUCTION

NASA is developing and demonstrating technologies to support future long-term human exploration missions beyond low-Earth orbit. A critical aspect of these missions is the storage and transfer of the cryogenic propellant. Liquid hydrogen and liquid oxygen provide the highest specific impulse of any practical chemical propellant, permitting longer range and higher payload mass. For long-duration missions, the cryogen storage tanks must be cooled to reduce or eliminate boil-off. Creare recently developed and delivered to NASA a single-stage turbo-Brayton cryocooler which will be used for thermal control of cryogen storage tanks. The required heat lift range for the cryocooler is 3 to 15 W of refrigeration at 77 to 90 K. The cryocooler will be used in separate ground demonstrations of: (1) reduced boil-off liquid hydrogen (LH2) storage; and (2) zero boil-off (ZBO) liquid oxygen (LOX) storage. The size of the cryogen storage tanks for these demonstrations will be nominally 1.5 m^3. Future space systems will utilize much larger cryogen storage tanks, which will require cryocoolers capable of lifting 100's of watts of heat. Turbo-Brayton cryocoolers are ideal for cooling cryogen storage tanks because they scale well to high capacities and can interface directly with a broad area cooling (BAC) systems located on cryogen tanks, eliminating the mass and input power penalty associated with a separate circulator.

Cryocoolers 17, edited by S.D. Miller and R.G. Ross, Jr.
©International Cryocooler Conference, Inc., Boulder, CO, 2012

The ZBO cryocooler delivered to NASA comprises components built for a prior flight program [1]. The components are evolved versions of the components in the NICMOS cryocooler that operated on the Hubble Space Telescope for 6.5 years [2]. The NASA project started on August 8, 2011; the cryocooler and interfaces with the cryogen storage tank were finalized on October 3, 2011; the cryocooler components were optimized and integrated; and the cryocooler completed thermal vacuum testing and was ready for delivery on February 13, 2012—nominally four months after finalizing the design. The cryocooler will be initially integrated at NASA Glenn Research Center (GRC) with a BAC on an actively cooled shield for the reduced boil-off LH2 demonstration. This demonstration is currently scheduled for the summer of 2012. The cryocooler will then be integrated and tested with a BAC on a LOX storage tank for the ZBO demonstration. This paper describes the cryocooler design, the interfaces with the cryogen storage tank, results from the cryocooler performance test conducted at Creare prior to delivery of the cryocooler, and scaling of the technology to higher cooling capacities.

CRYOCOOLER DESIGN

The NASA ZBO cryocooler is shown during integration at Creare in Figure 1. The working fluid is single-phase gaseous neon. A motor-driven compressor compresses the cycle gas from low to high pressure at the warm end of the system. The heat of compression is removed using an aftercooler. The heat of compression and losses associated with the compressor are rejected to space by a radiator (not shown). The compressor and aftercooler are mounted on a single interface plate and are connected to the rest of the cryocooler using flexlines to facilitate integration with the radiator at NASA-GRC. The high-pressure flow continues from the aftercooler through two recuperator modules where it is precooled by the low-pressure flow returning from the cold end. The flow then enters a turboalternator where refrigeration is produced by expansion of the cycle gas. The turbine mechanical work is converted to electric power by an alternator and is then transferred to ambient temperature where it is utilized by the electronics to control turbine speed and refrigeration load temperature. The cycle flow continues from the turboalternator to a load interface heat exchanger, which takes the form of a BAC system for cryogen storage applications. For testing at Creare, a BAC simulator was used to replicate the heat load and pressure drop associated with the BAC. A manifold at the cold end facilitates testing at Creare, delivery to NASA-GRC, integration with the BAC, and testing the integrated system, without the need to bake out the cryocooler after initial integration at Creare. The cold end manifold is shown in Figure 2.

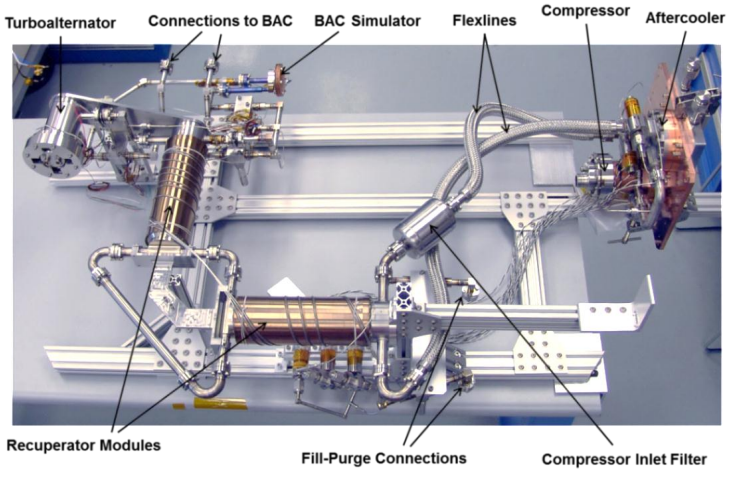

Figure 1. NASA ZBO cryocooler during preparation for thermal vacuum testing

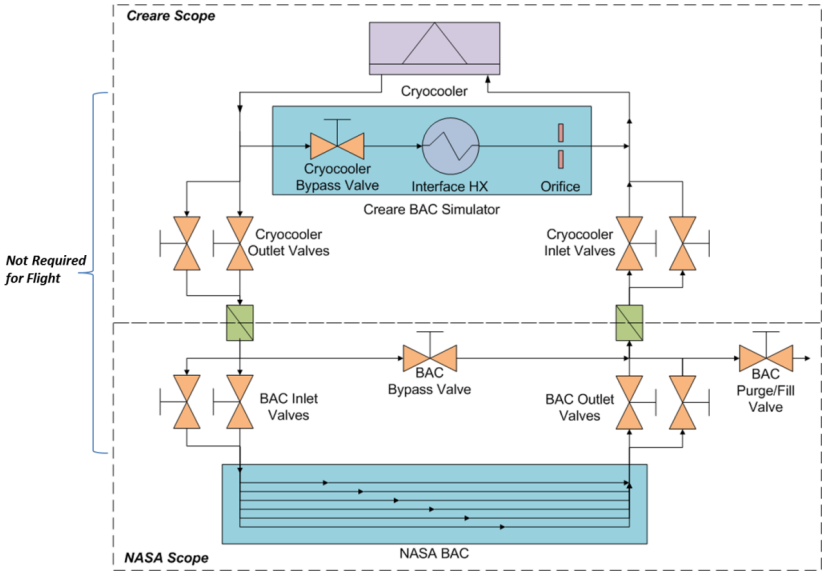

Figure 2. Cold end manifold used to connect cryocooler to broad area cooling system

The electronics (not shown in Figure 1) have flight-like functionality but utilize mostly rack-mounted, commercial components. Cryocooler control is fully automated via software and feedback loops managed by a digital signal processor. Warning and safing limits that protect the hardware are stored in non-volatile memory. High-level user commands are provided by a LabVIEW® interface, which also receives, processes, displays, and stores telemetry from instrumentation.

During testing at NASA, the cryocooler is mounted to an adapter ring that supports the cryogen tank. The compressor and aftercooler interface plate passes through an open space in the adapter ring and is mounted to a heat rejection radiator. Figure 3 shows the cryocooler mounted in the adapter ring at NASA GRC.

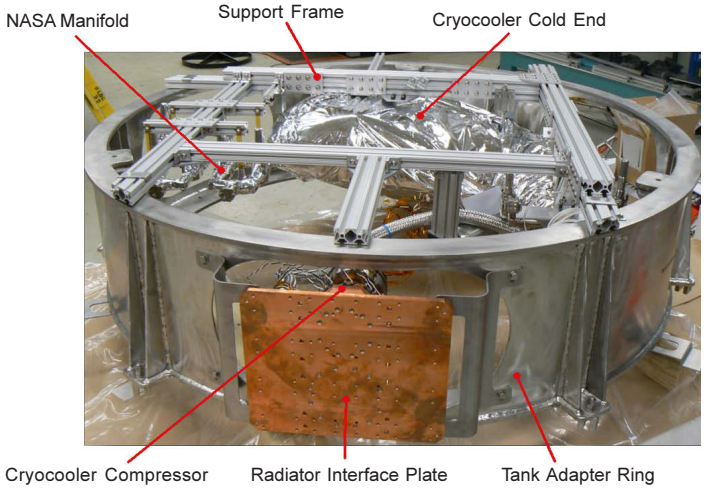

Figure 3. Cryocooler integrated into cryogen tank adapter ring

CRYOCOOLER TESTING AT CREARE

The cryocooler performance was measured at Creare through three separate cooldowns during February 2012. Figure 4 shows the cryocooler installed in the test chamber, and Figure 5 is a cycle schematic with pressure and temperature measurement locations. The cycle mass flow rate was determined from these measurements and the turboalternator flow resistance curve measured during component-level testing. The objectives of the tests were to characterize the thermodynamic performance of the cryocooler and verify functionality of the controls, telemetry, instrumentation, and mechanical hardware. The test data are described in subsequent sections. The error bars shown indicate the uncertainty of the measurement or derived quantity. Primary accomplishments of the test program include:

- Demonstrated autonomous start-up and cooldown
- Demonstrated operation of survival heaters
- Demonstrated set-point transitions (i.e., controls operated properly when new set-point temperature was commanded)
- Demonstrated excellent temperature regulation
- Verified mass flow rate prediction method
- Verified compressor AC power measurement
- Mapped performance of cryocooler at two load temperatures (80 K, 90 K) and two heat rejection temperatures (285 K, 300 K)
- Demonstrated cold shutdowns and re-starts

Data Quality Assessment

We reviewed the steady-state data for consistency and accuracy. The cold end temperature sensors are in-line sensors placed within the flow stream to limit systematic errors. The redundant BAC outlet temperatures (T7) agree to within 50 mK for all test points, which is within the band of their combined uncertainties (80 mK). The redundant turboalternator inlet temperatures (T5) and BAC inlet temperatures (T6) agree within nominally 250 mK. The poorer agreement for these redundant temperature sensors may be associated with a variation in the gas temperature in the vicinity of the turboalternator due to local heating. To mitigate this effect, we utilized the average of the redundant temperatures for calculating reduced parameters.

Figure 4. NASA ZBO cryocooler installed in test chamber at Creare

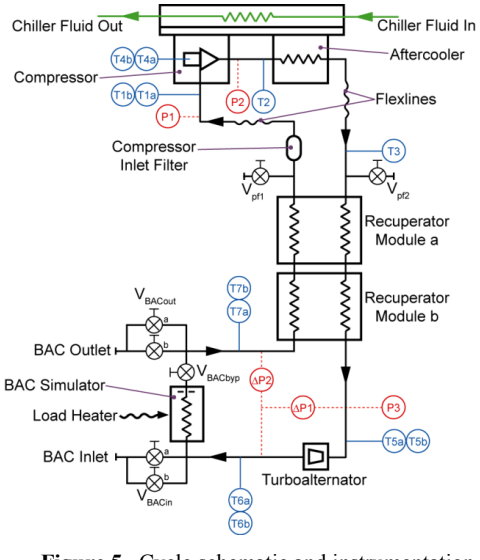

Figure 5. Cycle schematic and instrumentation locations

An energy balance on the BAC simulator and the turboalternator was used to assess the quality of the test data. Figure 6 compares the BAC heat load as determined from the BAC heater input power to the values determined from the enthalpy rise across the BAC simulator. The enthalpy rise method yields slightly greater values than the electrical power to the heater for most test points, though the agreement is within the uncertainty bars of the two methods. Similarly, Figure 7 compares the turbine refrigeration as determined from the electrical output power from the turboalternator to the enthalpy drop across the turboalternator. The electrical output power is greater than the enthalpy drop in all cases, which could be associated with thermal equilibrium effects (e.g., cold end temperature is still decreasing) or thermal parasitics from the environment. Regardless, the agreement for both the BAC heat load and turbine refrigeration is excellent, which provides confidence in our prediction of the mass flow rate. The uncertainty of the mass flow rate is nominally ± 3%.

We also performed an energy balance on the cold end at each test point. The results are shown in Figure 8. At steady state, the electrical power removed by the turboalternator is balanced by the sum of the net enthalpy flux from the recuperator (labeled as "Recuperator Loss" in Figure 8), the electrical power dissipated in the BAC heater, and thermal parasitics between the turboalternator inlet and BAC exit temperature sensors. The thermal parasitics are 0.56 ± 0.07 W for Test Points 6, 7, 11, and 12, which is consistent with our predictions for the sum of radiative parasitics through the multi-layer insulation (~ 0.44 W) and conductive parasitics through the cold end support (~ 0.14 W). These four test points were attained after several hours with the cold end at cryogenic temperatures and are believed to be free of transient effects. Overall, the energy balance indicates that the parasitics are modest and the data are consistent. The parasitics for Test Points 1–5 and 8–10 may have been impacted by transient effects associated with cooling the cold end. The amount of refrigeration associated with cooling the cold end is approximately the difference between the as-measured parasitics and the estimated parasitics (~ 0.56 W), which should only be weakly dependent on temperature for these test conditions. The transient cooling is significant for Test Points 1, 2, 8, and 9, and if these points were permitted to stabilize, then the input power is expected to be lower.

Cryocooler Performance

In Figure 9, the net refrigeration is plotted as a function of compressor AC input for three combinations of heat rejection temperature and BAC outlet temperature. The net refrigeration increases nominally linearly with compressor input power. The minimum and maximum heat loads applied at the BAC heater are 3 W and 15 W, respectively. At the nominal operating point of 9 W at 90 K, the cryocooler requires 213 W of net AC input power. The cryocooler has a maximum AC input power of nominally 400 W and can lift 20 W at 90 K at this power level.

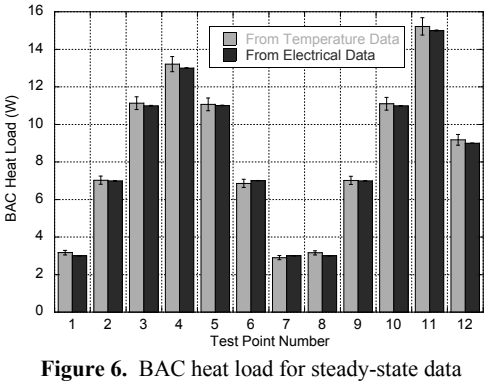

Figure 6. BAC heat load for steady-state data

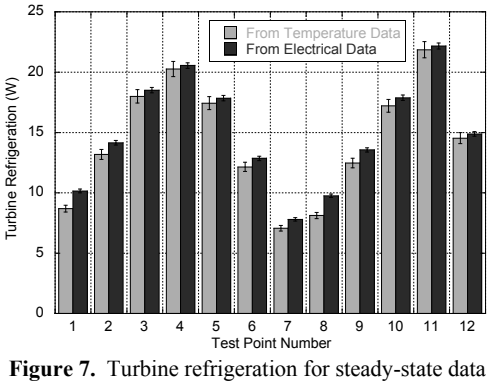

Figure 7. Turbine refrigeration for steady-state data

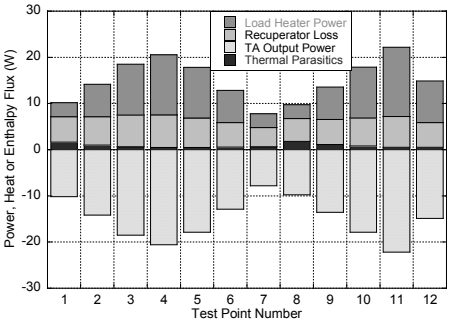

Figure 8. Cold end energy balance for steady-state data

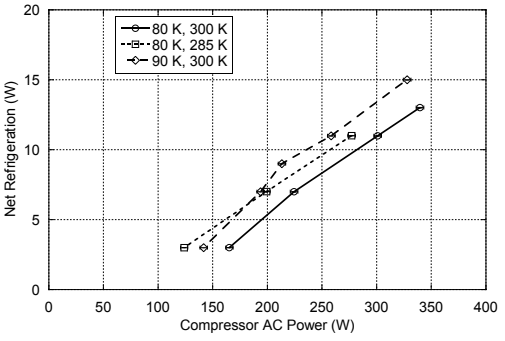

Figure 9. Net refrigeration for three combinations of heat rejection and load temperatures

The figure of merit for a cryocooler η_{Carnot} is the coefficient of performance (COP) for the cryocooler (cooling capacity divided by input power) divided by the COP of an ideal Carnot cycle operating at the same temperatures. That is:

$$\eta_{Carnot} = \frac{\dot{Q}_{net}}{\dot{P}_{AC,comp} - \dot{P}_{AC,TA}} \left(\frac{T_{reject}}{T_{load}} - 1 \right) \tag{1}$$

where $\dot{Q}_{net}$ is the net cooling load

$\dot{P}_{AC,comp}$ is the AC power into the compressor

$\dot{P}_{AC,TA}$ is the AC power from the turboalternator

T_{reject} is the heat rejection temperature[1]

T_{load} is the cooling load temperature[2]

The COP of the cryocooler relative to the Carnot cycle is shown in Figure 10. The Carnot efficiency increases with refrigeration capacity. The measured Carnot efficiency is 10.4% at the nominal operating point of 9 W at 90 K and 11.4% at the maximum load case of 15 W at 90 K.

The impact of heat rejection temperature is illustrated in Figure 11. Here the compressor input power is plotted as a function of heat rejection temperature (compressor inlet temperature for our tests) for three BAC heat loads at a BAC outlet temperature of 80 K. The compressor input power is slightly lower, and the Carnot efficiency of the cryocooler is slightly higher (see Figure 10) at the lower heat rejection temperature due primarily to the reduced work required to compress denser gas.

BAC Simulator

The BAC simulator was designed to simulate the pressure drop and heat loads of the BAC. The cryocooler was tested at Creare with the cryocooler inlet and outlet valves closed and sealed and the cryocooler bypass valve open (see Figure 2). The BAC simulator includes an orifice plate to replicate the pressure drop associated with the cryocooler inlet and outlet valves, BAC inlet and outlet valves, and tubing of the BAC (six parallel tubes of the BAC with 4.57 mm ID and a length of 5 m). The measured pressure drop for the BAC simulator as a function of mass flow rate is shown in Figure 12. The dissipation in the BAC heater is adsorbed by the cycle gas and increases its temperature. The temperature rise as a function of heater power is shown in Figure 13.

[1] The heat rejection temperature is taken to be the compressor inlet temperature.

[2] The load temperature is taken to be the BAC exit temperature.

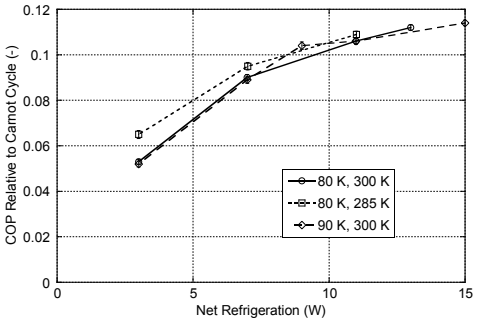

Figure 10. Cryocooler performance relative to the Carnot cycle

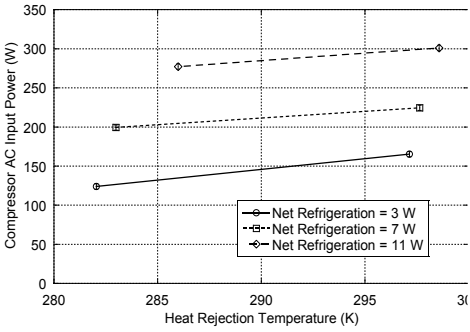

Figure 11. Impact of heat rejection temperatu with 80 K BAC outlet temperature

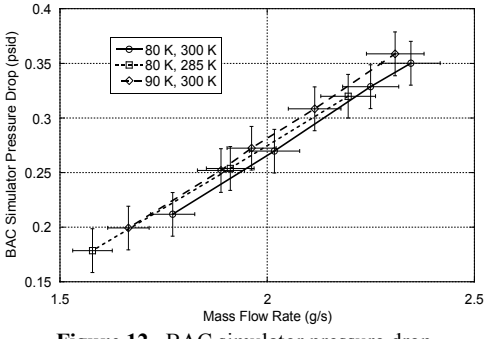

Figure 12. BAC simulator pressure drop

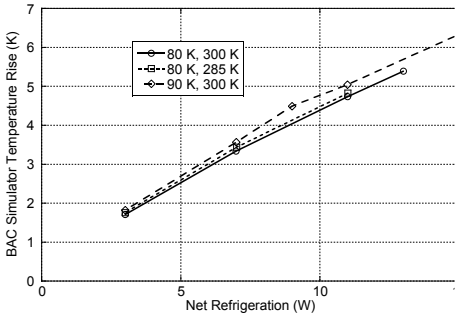

Figure 13. BAC simulator temperature rise

Temperature Regulation

The sequence of testing at Creare concluded with stabilizing at a cold end temperature of 90 K and a 9 W heat load. The temperature regulation during this period is shown in Figure 14, and the corresponding compressor AC input power is shown in Figure 15. The temperature regulation was better than ± 5 mK for a 300-minute period. The compressor input power decreased from 400 W to 213 W over the 550-minute period, where as the cold end temperature was within 100 mK of the set-point temperature during this period. The decrease in compressor power is indicative of the long period of time required to attain thermal equilibrium.

FLIGHT SYSTEM

The components and integration details for the ground test system were assessed to determine the mass and performance of a flight system of comparable capacity. The results are shown in Table 1. The projected mass for the flight system is 18 kg, as compared to 49 kg for the ground-test system. These values do not include the electronics, which have a flight weight of nominally 6 kg. The changes from the ground-test system to the flight system that impact mass are: (1) integration of the compressor and aftercooler into a single assembly; (2) integration of the recuperator modules and the turboalternator into a single assembly; (3) elimination of the cold end manifold; (4) replacement of the flexlines with rigid tubing with short, flexible elements as needed for integration; and (5) elimination of the aluminum support frame used to facilitate transportation, handling, and installation in the test chamber. These modifications were not implemented on the ground-test system for cost, schedule, and logistic reasons. The resulting flight cryocooler is shown in Figure 16.

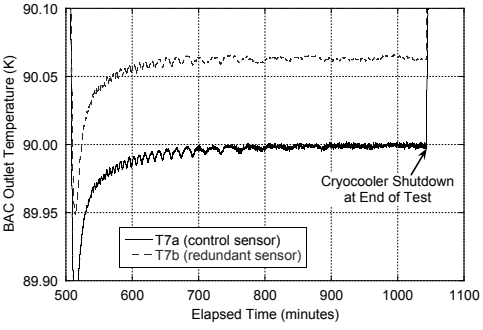

Figure 14. Temperature regulation at 90 K set-point

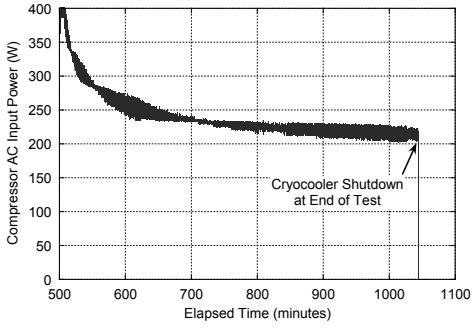

Figure 15. Compressor power during temperature regulation at 90 K set-point

Table 1. Cryocooler Scaling Comparison

Cryocooler Version	Ground Test 15 W at 90 K	Flight 15 W at 90 K	Flight 150 W at 90 K
Load Temperature	90 K	90 K	90 K
Heat Rejection Temperature	300 K	300 K	300 K
Compressor Pressure Ratio	1.56	1.56	1.56
Compressor Efficiency	42%	50%	55%
Turbine Efficiency	68%	75%	80%
COP Relative to Carnot	11.4%	14.7%	18.6%
Net AC Input Power (Compressor – TA)	306 W	237 W	1880 W
Mechanical Cryocooler Mass	49 kg	18 kg	116 kg
Mass per Cooling Capacity	3.3 kg/W	1.2 kg/W	0.77 kg/W

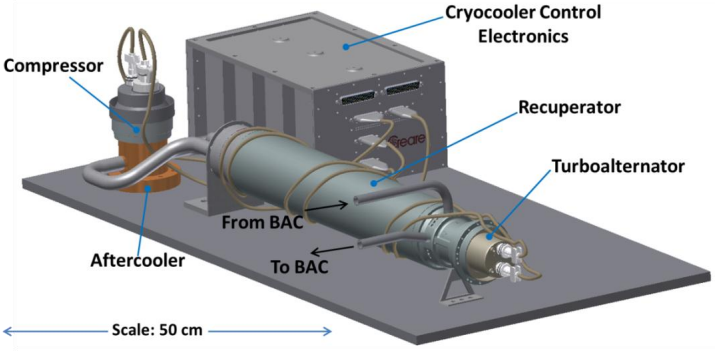

Figure 16. Flight turbo-Brayton cryocooler optimized for 15 W at 90 K

In addition, the cryocooler could be optimized for a flight system to reduce input power. The primary areas where the performance can be improved are the aerodynamic performance of the compressor impeller and turboalternator rotor and the losses in the compressor motor. The compressor and turboalternator utilized for this NASA program used legacy designs from the NICMOS program that were developed during the period of 1992 through 1995 [3]. Significant work has been performed at Creare to increase aerodynamic performance by using more advanced fabrication techniques and to develop permanent magnet motor compressors with lower losses than induction motors [4]. Compressor efficiencies of over 50% and turboalternator efficiencies of over 75% are expected at this power level with no change in cryocooler mass. The cryocooler input power is nominally inversely proportional to the compressor and turboalternator efficiency so that an increase in compressor efficiency from 42% to 50% and turboalternator efficiency from 68% to 75% will result in a 23% reduction in input power from 306 W of net AC power to 237 W. This reduction in input power corresponds to an increase in Carnot efficiency from 11.4% to 14.7% at the cooling capacity level of 15 W at 90 K. There is no additional development required to attain this reduction in input power.

SCALING TO HIGHER CAPACITIES

For future space missions, cooling capacities higher than 15 W at 90 K will be required for LOX storage tanks. With test data and mass properties in hand, we performed a scaling study for a high-capacity flight cryocooler providing 150 W of refrigeration at 90 K. Requirements for space sensor cooling have driven turbo-Brayton technology development toward miniaturization of precision components in order to achieve good thermodynamic cycle performance at low cooling loads. However, the turbo-Brayton cycle is inherently a high-capacity system. The high operating speeds of the turbomachines allow high power in a compact, lightweight package, and the overhead losses associated with the high operating speeds become a small fraction of the input power at high capacities. The result is that the efficiency increases and the specific mass (mass per cooling capacity) decreases in comparison to other cryocooler options as the refrigeration capacity increases [5].

The results of our scaling study are shown in Table 1. The “cryocooler versions” in Table 1 correspond to the demonstrated cryocooler, a modest-capacity flight cryocooler (15 W at 90 K), and a high-capacity flight system (150 W at 90 K). For the high-capacity system, the efficiency of the compressor and turboalternator will be higher because the overhead losses will be a smaller fraction of the aerodynamic power. The recuperator loss and thermal parasitics will be a smaller fraction of the turboalternator output power because these losses scale with surface area to volume ratio which is decreasing with increasing capacity. The cryocooler mass is scaled with input power to an exponent of 0.9. An exponent of less than one reflects that the mass of the components have an overhead fraction that does not scale with power level. The result is that a high-capacity cryocooler could be developed that provides 150 W of refrigeration at 90 K with 1880 W of net AC input power. The Carnot efficiency of this system is 18.6%, and the mass is 116 kg.

This high capacity system is within the range of prior work at Creare. For example, Creare has developed and demonstrated a 2.5 kW compressor for an airborne application. This compressor is liquid-cooled and was driven by a high-speed machine tool inverter. The compressor would need to be modified for conductive cooling typical of space applications, and high power space electronics would need to be developed. There has been considerable work on high power space electronics for turbo-Brayton systems at NASA for space nuclear propulsion systems. This work is directly applicable to the power electronics in turbo-Brayton cryocoolers. In addition, a new turboalternator would need to be developed for high capacity space applications. We have developed and demonstrated turboalternators for airborne applications with refrigeration capacities up to 2 kW at 100 K and for space-borne applications with refrigeration capacities of 30 W at 100 K. We recently built a 2.5 kW turboalternator for a terrestrial application. This turboalternator is a scaled version of our space-borne turboalternators. A recu-

perator would also need to be developed, though this would likely be a space-quality version of a commercial plate-fin recuperator.

SUMMARY

A single-stage turbo-Brayton cryocooler was developed and tested by Creare and delivered to NASA for use in ground demonstrations of reduced and zero boil-off cryogen storage. The cryocooler was developed on an accelerated schedule using mostly components built on a prior program. The time from finalization of design to having the cryocooler being ready for delivery was nominally four months. Thermal vacuum testing of the cryocooler at Creare confirmed that it met all performance and operational requirements. The cryocooler demonstrated 15 W of refrigeration at 90 K with 306 W of input power. A flight version of the cryocooler was also assessed that is lighter and more efficient using the most current component technology. A higher capacity cryocooler providing 150 W of refrigeration at 90 K was also studied. This cryocooler would comprise developmental components and is intended for large-scale cryogen storage consistent with future long-term human exploration missions beyond low-Earth orbit.

ACKNOWLEDGMENT

The support and guidance of NASA and AFRL are gratefully acknowledged.

REFERENCES

1. Zagarola, M.V., Breedlove, J., Kirkconnell, C.S., Russo, J.T., and Chiang, T., "Demonstration of a Two-Stage Turbo-Brayton Cryocooler for Space Applications," *Cryocoolers 15*, edited by S.D. Miller and R.G. Ross, Jr., ICC Press, Boulder, CO, 2009, pp. 461-469.
2. Swift, W.L., Dolan, F.X., and Zagarola, M.V., "The NICMOS Cooling System—5 Years of Successful On-Orbit Operation," *Adv. in Cryogenic Engineering*, Vol. 53, Amer. Institute of Physics, Melville, NY (2008), pp. 799-806.
3. Dolan, F.X., Swift, W.L., Tomlinson, B.J., Gilbert, A., and Bruning, J., "A Single Stage Reverse Brayton Cryocooler: Performance and Endurance Tests on the Engineering Model," *Cryocoolers 9*, edited by R.G. Ross, Jr., Plenum Press, New York, NY, 1997, pp. 465-474.
4. Hill, R.W., Hilderbrand, J.K., and Zagarola, M.V., "An Advanced Compressor for Turbo-Brayton Cryocoolers," *Cryocoolers 16*, edited by S.D. Miller and R.G. Ross, Jr., ICC Press, Boulder, CO, 2011, pp. 391-396.
5. Zagarola, M., and McCormick, J., "High-Capacity Turbo-Brayton Cryocoolers for Space Applications," *Cryogenics*, Vol. 46, No. 2-3, 2005, pp. 169-175.